Proceedings of DETC'00
ASME 2000 Design Engineering Technical Conferences and Computer and Information in Engineering Conference
Baltimore, Maryland, September 10-13, 2000

DETC2000/DAC-14271

TUBE PRODUCTION AND ASSEMBLY SYSTEMS: THE IMPACT OF COMPLIANCE AND VARIABILITY ON YIELD

Yu-Feng Wei
Graduate Research Assistant
Department of Mechanical Engineering
Massachusetts Institute of Technology
Cambridge, MA 02139

Anna C. Thornton
Assistant Professor
Department of Mechanical Engineering
Massachusetts Institute of Technology
Cambridge, MA 02139

ABSTRACT

Variation modeling is used in design to predict and diagnose potential quality problems. Most variation modeling assumes the parts are rigidly assembled. However, in some cases, this assumption is invalid. For example, when hydraulic tubes are assembled into aircraft structures, the compliance of the tube facilitates assembly. If the tubes were rigid, they cannot be assembled, i.e., the variations of the tubes and structures are too great. Despite the importance of compliance in assembly, it is typically not explicitly modeled during design. This paper proposes a new method to directly predict the assemblability of any tube design with minimal dependence CAD/FEM modeling and simulation. The model includes a variation model for the tubes and aircraft, compliance model and assembly model. It can be used during design to improve yields.

1. INTRODUCTION

Tubes are extensively used in sophisticated vehicles such as aircraft and submarines for hydraulic control systems, airflow systems, and waste systems. Because of the functional requirement of transporting substances through a complex structure, tubes are typically bent into complex shapes.

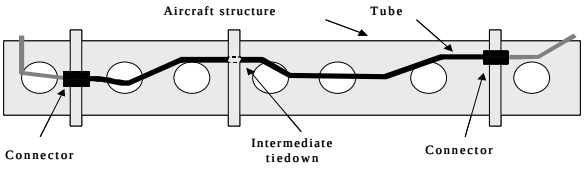

Figure 1: Example of assembled tube

Figure 1 shows a typical hydraulic tube in an aircraft. The tube ends are connected to either a structural part on the aircraft or another tube. It must pass through holes in the structure and bend around obstructions. In addition, the tube is typically *tied-down* at a series of points. These tie-downs prevent vibration, ensure the proper location of the tubes, and provide structural support. In general, there is variation in connection points, tie-down points and the tube. The assembler must apply force and moment loads to fit the tube into the install points. Because the tube has bends, a large aspect ratio, and is thin-walled, the tube compliance is typically used to enable assembly. However, putting load on the tube can impact the life-cycle performance of the tubes. As a result, a maximum load is specified. If a tube cannot be installed without exceeding that load, the tube is rejected. Figure 2 shows that the assembly with geometrical variations in both tube and structure requires assembly loads.

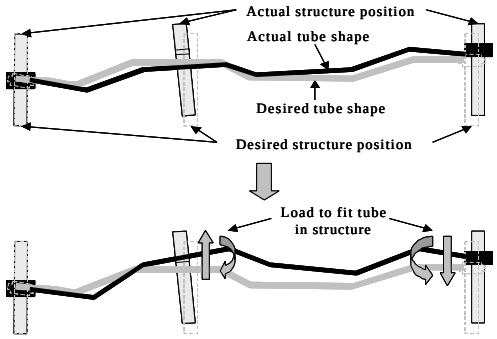

Figure 2: Variations in tube assembly and the assembly loads

There are a number of ways to increase the install yields of tubes: variation reduction (reducing the sources of variation in the tubes and the aircraft), design changes (increasing the robustness to process variations; increasing the compliance of the part), and inspection before installation. In order to quantify and evaluate their effects on yield, the alternatives need to be modeled simultaneously to ensure the optimum approach. For example, manufacturing variation reduction and inspection are the popular approaches for quality management. However, in this paper we demonstrate that inexpensive design change can significantly improve the yield.

The authors are developing a set of tools to help design the optimal production systems for tube manufacture. This paper describes the first part of the research: a set of systematic methods to model the impact of variability and compliance on install yields.

Several methods can be used for variability and compliance analysis. Monte Carlo simulation, numerical methods and FEM are often the *de facto* modeling approaches for them. However, the problem of such analysis provides several interesting challenges. For instance, in a typical aircraft there are thousands of unique tubes. In order to analyze each tube, it would be necessary to individually model and analyze its geometry. Using FEM packages plus simulation would not be feasible given the large number of parts.

This research presents a direct method to calculate the probability of rejection, given the manufacturing variability (in both tube and aircraft) and the compliance of the tube. We use matrix operations to derive the tube compliance instead of FEM software. Furthermore, this method uses the digital definition of the tube (i.e., the bend plan) as the input. As a result, no CAD/FEM models are necessary and thus the modeling and computational efforts are minimized. These models are programmed in MS Excel, and the CPU time for geometry and compliance computation is about 20 seconds with a Pentium II 266 processor with 128M RAM. This research sets out to answer three questions.

How do the bending process variations affect the tube geometry? Given the process variations of the bending machine and other operations, it is necessary to understand how the final shapes of single tube and a population of tubes deviate from its nominal geometry. This is described in Section 3.3.

How can tube compliance be predicted? FEM is computationally expensive, thus not feasible for this process. For simple-geometry components, compliance can be calculated directly through matrix operations. This method significantly reduces the modeling and computational efforts, relative to FEM. This is described in Section 3.4.

How is assembly yield computed? Once the variability and compliance of the part are modeled, the next step is to link them with the acceptance criteria in assembly. Expected assembly yield can be calculated analytically or estimated statistically through simulation. This information can be used as feedback for tube design, process capability, and production planning. This is described in Section 3.5.

2. RELATED WORK

Research in the area of variation modeling and yield prediction falls into several categories. One group of researchers focuses on manufacturing processes. Kazmer *et al.* (1996) use predictive model to analyze part variation and robustness in the injection molding process. Frey (1997) proposes the Process Capability Matrix method to propagate variations of multiple quality characteristics and predict the yield in multiple operations manufacturing. Suri and Otto (1999) present the Integrated System Model method that predicts variations in manufacturing system, and provides a feed-forward control scheme for the stretch forming process. These methods focus on modeling the effects of operational settings and variations in manufacturing processes on the variations of part features. A similar approach is used in this paper to model the variation in tube bending process.

Another group of researchers focuses on variation and tolerance analysis in assembly. Previous works include geometric representation and variation stack-up. Guilford and Turner (1993) summarize the geometric representation techniques into three categories: parameter space, solid offset, and feasibility space. Many researchers (e.g., Daniel *et al.* 1986, Turner 1990, Takahashi 1991) use Monte Carlo simulation or numerical methods to propagate variation in assembly. Simulation-based commercial software is also available (e.g. VSA-3D). Turner and Gangoiti (1991) present a comprehensive survey on these commercial packages. Bjorke (1978) uses a statistical approach for one-dimensional variation stack-up in tolerance analysis. Based on the work by Veitschegger and Wu (1986), Whitney *et al*. (1994) extend the statistical approach to the 3-D case by incorporating the homogeneous transform matrix (HTM) for geometric representation. Their method predicts the spatial distribution of position and orientation of parts during assembly, and calculates the yield analytically. In this paper we modify this method and apply it to the tube bending model. Most of the preceding research has the assumption of rigid parts, and does not consider part deformation during process and assembly.

Only a few works exist for the variation modeling of compliant part assembly. Liu and Hu (1997) point out that the combination of Monte Carlo simulation with FEM is very computationally intensive. They derive the variation propagation equation for sheet metal assembly with reduced FEM requirement and use Monte Carlo simulation to attain the variation distribution. Hu (1997) also proposes "stream of variation" theory for variation propagation and diagnosis for compliant sheet metals in the auto body assembly process. Their approach still replies on FEM modeling, which is not feasible for high-variety parts.

Another group of researchers focuses on the design optimization of pipe/tube routing. Szykman and Cagan (1996) summarize them and propose a synthesis method based on the simulated annealing algorithm. However, their method only considers direct costs, such as material cost and bending cost. Variation and quality related costs are not addressed.

In summary, there is a lack of efficient variation-modeling approach for compliant parts from the manufacturing process to assembly. Our research strategy will incorporate current techniques in variation modeling for 3-D rigid parts and solid mechanics with minimum computational requirement.

3. MODELING METHODS

In this section we present the tube modeling methods. We first describe the methods used by industry, in which tubes are described in terms of bend plans sent to the tube bender. Secondly, we describe how this plan can be used to describe the 3-D geometry of the tube. Then based on the 3-D geometry model, we present the mathematical models for geometrical variation and characteristic compliance of tubes. Lastly, we introduce methods that incorporate these models to predict the tube assembly yield.

3.1. Bending model

Tubes are built through a cold forming process. This process is a single-machine-multi-operation tube bending process that transforms straight raw tubes into desired three-dimensional shapes.

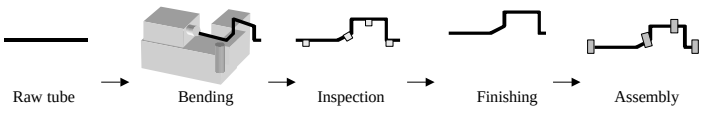

Figure 3: Typical tube bending production and assembly processes

A tube is uniquely described by the specifications of raw tube and the bend plan. The specifications include material, diameter, wall thickness and length. The bend plan is composed of a series of triplets. Each triplet describes the length between bends (shoot), the angle of rotation (rotate) and the angle of bend (bend). In addition, the bend radius is set by the forming die and is the same for all bends. Figure 4 shows these values and the global coordinate system[1] that will be used throughout the paper.

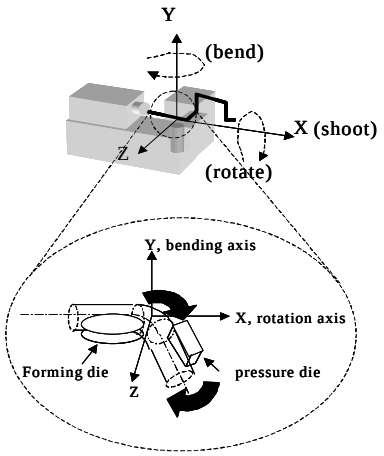

Figure 4: Global coordinate system XYZ and the three motions in a bend cycle

Shooting is a translation along the **X**-axis by an amount l, rotation is a negative rotation around the **X**-axis by an amount b, and bending is a negative rotation around the **Y**-axis by an amount a. Each bend cycle is a three-step coordinate transformation comprising one translation and two rotations of the bent part of the tube. Figure 5 shows the complete process and the three variables in a single bend cycle.

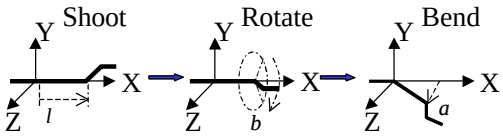

Figure 5: Tube bending process and process variables

3.2. Tube Geometry model

From the bend plan it is possible to generate the geometry of the tube in 3-D space. This is done using the Homogeneous Transformation Matrix (HTM) to transform the location and orientation of the bends as the bend plan is executed.

To simplify the modeling, we break the model into two parts. In the first model, the linear centerline model, we represent the tube as if the bending radius was zero (i.e., all sections are straight). We predict for each bend the theoretical breakpoint: the location of the bend if the bending radius is zero. The linear centerline model enables us to simplify the variation propagation model. The second model, the curvilinear centerline model, includes the bending radius. The curvilinear model is used to more accurately predict the compliance. In both cases, we only model the centerline of the tube; we assume that the tube diameter is zero and we are bending only the centerline. In addition, we assume that the

[1] The global coordinate system is attached to the bender.

variation introduced by the tube diameter is insignificant and can be ignored. Figure 6 shows both representations.

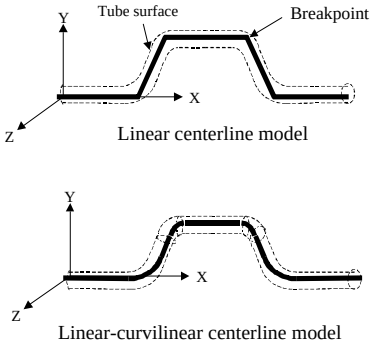

Figure 6: Representation of tube geometry

The overall shape of a tube can be described by the 3-D positions of all breakpoints plus the two end points in the global coordinate system, as shown in Figure 7. There are *n* bends and point ***u*** is an arbitrary point on the tube centerline. We will use this representation throughout our model derivation.

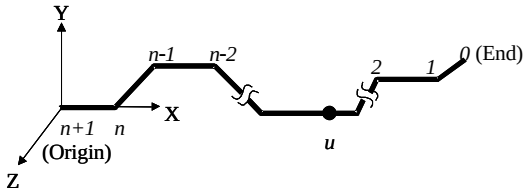

Figure 7: Representation of tube geometry in global coordinate system

We locate these points by setting point *n+1* as the origin (the left end of the tube) and calculating the HTM for each bend cycle. When the i^{th} bend is created, point ***u*** undergoes the following coordinate transformation.

$$ {}^{i}\mathbf{T}_{i-1} = \begin{pmatrix} \cos a_i & \sin a_i \sin b_i & -\sin a_i \cos b_i & l_i \cos a_i \\ 0 & \cos b_i & \sin b_i & 0 \\ \sin a_i & -\cos a_i \sin b_i & \cos a_i \cos b_i & l_i \sin a_i \\ 0 & 0 & 0 & 1 \end{pmatrix} \quad \text{Eq (1)} $$

The effect of multiple bends can be combined into one HTM through a series of matrix multiplications. The following HTM is the total transformation matrix from the i^{th} to the $(n+1)^{th}$ bend cycle:

$$ \mathbf{T}_i = {}^{n+1}\mathbf{T}_n * {}^{n}\mathbf{T}_{n-1} * \cdots * {}^{i+1}\mathbf{T}_i = \begin{pmatrix} \mathbf{R}_i & \mathbf{P}_i \\ \mathbf{0} & 1 \end{pmatrix} \quad \text{Eq (2)} $$

Later in the paper we will use parts of the total transformation matrix to calculate variation propagation. These parts are the 3x3 rotational matrix $\mathbf{R}_i$ and the 3x1 translational vector, $\mathbf{P}_i$. [2]

The linear-curvilinear centerline model can be derived from the linear centerline model by plugging in the curvilinear sections and calculating the tangent points. Figure 8 illustrates the procedure.

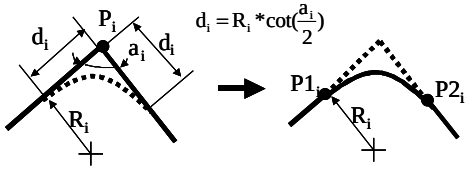

Figure 8: Conversion of linear-curvilinear centerline model

3.3. Variation Propagation

Now that we have described the 3-D shape in global coordinate system, the HTM $\mathbf{T_i}$ can be used to calculate the impact of process variation on the resultant geometry. Each shoot, bend, and rotation introduces variation into the geometry. For example, the effect of gravity makes the tubes sag making the rotation less accurate; springback and material variation introduces variation into the bends; errors in indexing, slip and other machine problem introduce errors in the shoot. These errors are contained in a vector, **V**.

By using linear approximation, we will derive the relation between the process errors, **V,** and the geometrical errors, **U,** in the following form:

$$ \mathbf{U} = \mathbf{S} * \mathbf{V} \quad \text{Eq (3)} $$

Vector **U** is the complete set of geometrical errors in six degrees of freedom at all points of interest on the tube. Vector **V** is the complete set of process errors in shooting, bending, and rotating. **S** is the process sensitivity matrix. The following section derives **S** from the HTM matrices. For simplification, we will demonstrate the derivation at one point on the tube, ***u***, as shown in Figure 7.

The geometrical error at an arbitrary point ***u*** contains two parts, translational error $d\mathbf{P}=(dx, dy, dz)^T$ and rotational error $\mathrm{d}=(dx, dy, dz)^T$. The bending machine introduces a set of errors affecting point ***u*** during the *m* bend cycles[3] that make

[2] Note that ${}^{n+1}\mathbf{T}_n$ is the HTM from the last breakpoint to the origin of XYZ with translation of ln+1 only ($a_{n+1} = b_{n+1} = 0$).

[3] If u locates between the $(j-1)^{th}$ and j^{th} breakpoints, m equals $(n-j+1)$, i.e., $(n-j)$ bends plus the last straight section.

the bends between point ***u*** and the end of tube that we choose as the origin. These errors are denoted as $d\mathbf{l}=(dl_1, dl_2,\ldots,dl_m)^T$, $d\mathrm{a}=(da_1, da_2,\ldots,da_m)^T$ and $d\mathrm{b}=(db_1, db_2,\ldots, db_m)^T$. The geometrical and process errors can be linked through the following linear equations (Veitschegger 1986; Whitney 1994):

$$\begin{pmatrix} d\mathbf{P} \\ \mathbf{d} \end{pmatrix} = \begin{pmatrix} \mathbf{W}_1 & \mathbf{W}_2 & \mathbf{W}_3 \\ \mathbf{0} & \mathbf{W}_4 & \mathbf{W}_5 \end{pmatrix} * \begin{pmatrix} d\mathbf{l} \\ d\mathbf{a} \\ d\mathbf{ß} \end{pmatrix} \qquad \text{Eq (4)}$$

Where $\mathbf{W}_1$ through $\mathbf{W}_5$ are 3x*m* sensitivity matrices.[4] The derivation of $\mathbf{W}_1$ through $\mathbf{W}_5$ is explained below.

Consider a point ***u*** located between point *j-1* and *j* (*j*<*i*), as shown in Figure 9. The process errors dl_i, da_i and db_i contribute to the translational and rotational errors at the point of interest ***u*** through the following relationship.

$$\mathbf{d}_i = \mathbf{R}_i * \begin{pmatrix} -db_i \\ -da_i \\ 0 \end{pmatrix} \qquad \text{Eq (5)}$$

$$d\mathbf{P}_i = \mathbf{R}_i * \begin{pmatrix} dl_i \\ 0 \\ 0 \end{pmatrix} + \mathbf{d}_i \times (\mathbf{R}_i * {}^i\mathbf{P}_u) \qquad \text{Eq (6)}$$

In the equation above, ${}^i\mathbf{P}_u$ is the 3x1 translational vector from i^{th} breakpoint to point ***u*** in the global coordinate system when i^{th} bend cycle is to be executed. It can be obtained through the following equation:

$${}^i\mathbf{T}_u = {}^i\mathbf{T}_{i-1} * {}^{i-1}\mathbf{T}_{i-2} * \cdots * {}^j\mathbf{T}_u = \begin{pmatrix} {}^i\mathbf{R}_u & {}^i\mathbf{P}_u \\ \mathbf{0} & 1 \end{pmatrix} \qquad \text{Eq (7)}$$

In Eq (7), ${}^j\mathbf{T}_u$ equals ${}^j\mathbf{T}_{j-1}$ with l_u replacing l_j. The product vector of $\mathbf{R}_i * {}^i\mathbf{P}_u$ is the translational vector from the i^{th} breakpoint to ***u*** in the global coordinate system when the last bend cycle is finished. The last term of Eq (6) is the Abbe error caused by the rotational errors at the i^{th} breakpoint.

[4] The rotational error vector is determined only by rotational errors in bending process, while the positional error vector is determined by both translational and rotational errors.

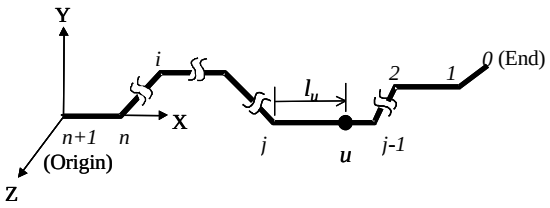

Figure 9: Arbitrary point *u* on the tube

Since we assume the errors to be small, the total geometrical errors can be obtained by summing up the errors introduced by individual bend cycles. Therefore,

$$\mathbf{d} = \sum_{i=j}^{n+1} \mathbf{d}_i^u \qquad \text{Eq (8)}$$

$$d\mathbf{P} = \sum_{i=j}^{n+1} d\mathbf{P}_i^u \qquad \text{Eq (9)}$$

By summarizing Eq (5), (6), (8) and (9), we can express Eq (4) through the following equations:

$$\mathbf{W}_1 = \begin{pmatrix} \mathbf{R}_j^1 & \mathbf{R}_{j+1}^1 & \cdots & \mathbf{R}_{n+1}^1 \end{pmatrix}$$

$$\mathbf{W}_2 = -\begin{pmatrix} \mathbf{R}_j^2 \times (\mathbf{R}_j * {}^j\mathbf{P}_u) & \mathbf{R}_{j+1}^2 \times (\mathbf{R}_{j+1} * {}^{j+1}\mathbf{P}_u) & \cdots & \mathbf{R}_{n+1}^2 \times (\mathbf{R}_{n+1} * {}^{n+1}\mathbf{P}_u) \end{pmatrix}$$

$$\mathbf{W}_3 = -\begin{pmatrix} \mathbf{R}_j^1 \times (\mathbf{R}_j * {}^j\mathbf{P}_u) & \mathbf{R}_{j+1}^1 \times (\mathbf{R}_{j+1} * {}^{j+1}\mathbf{P}_u) & \cdots & \mathbf{R}_{n+1}^1 \times (\mathbf{R}_{n+1} * {}^{n+1}\mathbf{P}_u) \end{pmatrix}$$

$$\mathbf{W}_4 = -\begin{pmatrix} \mathbf{R}_j^2 & \mathbf{R}_{j+1}^2 & \cdots & \mathbf{R}_{n+1}^2 \end{pmatrix}$$

$$\mathbf{W}_5 = -\mathbf{W}_1$$

where $\mathbf{R}_j^1$ represents the first column (3x1 vector) and $\mathbf{R}_j^2$ is the second column of $\mathbf{R}_j$.

To derive the complete variation propagation equation as Eq (3), the procedures are repeated to obtain the variation propagation equations for all points of interest and organize them into matrix form.

3.4. Compliance

The load required to overcome the tube and aircraft variation is determined by the compliance of the tube. By predicting the required loads and comparing them to maximum allowance, the yield rates during assembly can be determined.

Compliance is represented by the stiffness matrix. This section derives the characteristic stiffness matrix, **K**, which linearly maps the generalized displacements (geometrical errors), **X,** to generalized forces (assembly loads), **F,** required

to assemble the part into the tiedown points. The stiffness matrix is symmetric and independent of the assembly process according to Betti's reciprocal theorem.

$$\mathbf{F} = \mathbf{K} * \mathbf{X} \qquad \text{Eq (10)}$$

Where [5] $\mathbf{F} = (\mathbf{F_1}, \mathbf{F_2}, \cdots, \mathbf{F_h})^T$ and $X = (\mathbf{X_1}, \mathbf{X_2}, \cdots, \mathbf{X_h})^T$. **X** is the set of geometrical errors including **U** (geometrical errors in tube) and **U'** (geometrical errors in structure) at all points of interest.

$$\mathbf{X} = \mathbf{U} + \mathbf{U}' \qquad \text{Eq (11)}$$

Three approaches can be applied to model the stiffness matrix (Chang 1996): For parts with simple geometry such as beams, blocks, and rings, it can be obtained by solving the set of differential equations of equilibrium. For parts that can be dissected and approximated by elements with simple geometry, it can be calculated directly through matrix operations on the stiffness matrices of its components. For parts with complex geometry, it must be modeled by FEM. Since a tube can be modeled as a series of linear and curvilinear thin-wall cylinders, the second approach is adopted.

The modeling procedure starts with dissecting the tube into linear and curvilinear sections. These sections are further divided at the points of interest. Their stiffness matrices can be obtained directly from the formulae handbook for structural elements (straight and circular thin-wall beams). In this paper the formulae are obtained from Pilkey's (1994) handbook. The next step is applying matrix operations to condense the section stiffness matrices and compose them into global stiffness matrix. An example in Figure 10 illustrates the process.

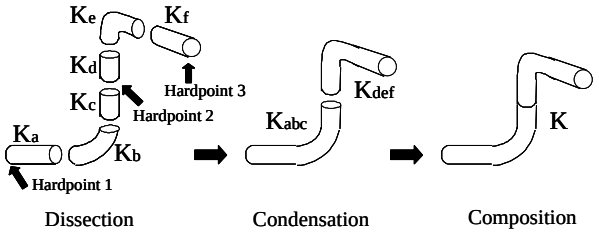

Figure 10: Procedure to compose global stiffness matrix

In the example above, we want to derive the stiffness matrix that links the generalized forces and generalized displacements on the three hardpoints. We first find the section stiffness matrices $\mathbf{K_a}$ through $\mathbf{K_c}$, which are three 12x12 matrices comprising six plus six degrees of freedom on both ends (2 nodes) of each section. They can be obtained directly from formula tables (Pilkey 1994) for straight and circular beam. Next we derive the stiffness matrix $\mathbf{K_{abc}}$, which is a 12x12 matrix comprising six plus six degrees of freedom on hardpoint 1 and 2. It can be obtained by condensing $\mathbf{K_a}$ through $\mathbf{K_c}$. Similarly, $\mathbf{K_{def}}$ is a 12x12 matrix comprising six plus six degrees of freedom on hardpoint 2 and 3, and can be obtained by condensing $\mathbf{K_d}$ through $\mathbf{K_f}$. The condensation process is illustrated below.

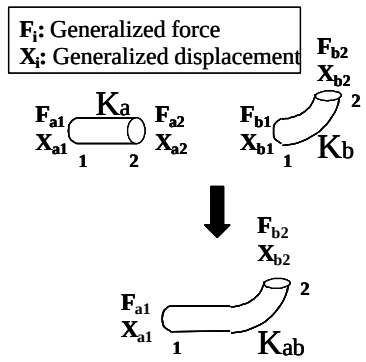

Figure 11: Illustration of stiffness matrix condensation

As shown in Figure 11, the second node of $\mathbf{K_a}$ is to be merged with the first node of $\mathbf{K_b}$, and the degrees of freedom on the node are to be eliminated (generalized force on the merging node is zero). Let $\mathbf{K_a} = \begin{pmatrix} \mathbf{K_{a11}} & \mathbf{K_{a12}} \\ \mathbf{K_{a12}^T} & \mathbf{K_{a22}} \end{pmatrix}$ and $\mathbf{K_b} = \begin{pmatrix} \mathbf{K_{b11}} & \mathbf{K_{b12}} \\ \mathbf{K_{b12}^T} & \mathbf{K_{b22}} \end{pmatrix}$, where $\begin{pmatrix} \mathbf{F_{a1}} \\ \mathbf{F_{a2}} \end{pmatrix} = \begin{pmatrix} \mathbf{K_{a11}} & \mathbf{K_{a12}} \\ \mathbf{K_{a12}^T} & \mathbf{K_{a22}} \end{pmatrix} * \begin{pmatrix} \mathbf{X_{a1}} \\ \mathbf{X_{a2}} \end{pmatrix}$ and $\begin{pmatrix} \mathbf{F_{b1}} \\ \mathbf{F_{b2}} \end{pmatrix} = \begin{pmatrix} \mathbf{K_{b11}} & \mathbf{K_{b12}} \\ \mathbf{K_{b12}^T} & \mathbf{K_{b22}} \end{pmatrix} * \begin{pmatrix} \mathbf{X_{b1}} \\ \mathbf{X_{b2}} \end{pmatrix}$. By solving $\mathbf{F_{a2} + F_{b1} = 0}$ and $\mathbf{X_{a2} = X_{b1}}$, the constitutive relation for the two-part system can be rewritten as $\begin{pmatrix} \mathbf{F_{a1}} \\ \mathbf{F_{b2}} \end{pmatrix} = \mathbf{K_{ab}} * \begin{pmatrix} \mathbf{X_{a1}} \\ \mathbf{X_{b2}} \end{pmatrix}$, where $\mathbf{K_{ab}} = \begin{pmatrix} \mathbf{K_{a11} - K_{a12} * (K_{a22} + K_{b11})^{-1} * K_{a12}^T} & \mathbf{-K_{a12} * (K_{a12} + K_{b11})^{-1} * K_{b12}} \\ \mathbf{-K_{b12}^T * (K_{a22} + K_{b11})^{-1} * K_{a12}^T} & \mathbf{K_{b22} - K_{b12}^T * (K_{a22} + K_{b11})^{-1} * K_{b12}} \end{pmatrix}$, yielding a 12x12 matrix. By repeating this procedure, $\mathbf{K_{ab}}$ and $\mathbf{K_c}$ can be condensed into $\mathbf{K_{abc}}$.

The final step is to derive the global stiffness matrix **K**, which is an 18x18 matrix that has six degrees of freedom on the three hardpoints and can be obtained from $\mathbf{K_{abc}}$ and $\mathbf{K_{def}}$. Let $\mathbf{K_{abc}} = \begin{pmatrix} \mathbf{K_{abc11}} & \mathbf{K_{abc12}} \\ \mathbf{K_{abc12}^T} & \mathbf{K_{abc22}} \end{pmatrix}$ and $\mathbf{K_{def}} = \begin{pmatrix} \mathbf{K_{def11}} & \mathbf{K_{def12}} \\ \mathbf{K_{def12}^T} & \mathbf{K_{def22}} \end{pmatrix}$, then $\mathbf{K} = \begin{pmatrix} \mathbf{K_{abc11}} & \mathbf{K_{abc12}} & \mathbf{0} \\ \mathbf{K_{abc12}^T} & \mathbf{K_{abc22} + K_{def11}} & \mathbf{K_{def12}} \\ \mathbf{0} & \mathbf{K_{def12}^T} & \mathbf{K_{def22}} \end{pmatrix}$, in which the second node of $\mathbf{K_{abc}}$ and the first node of $\mathbf{K_{def}}$ are superimposed.

[5] Note that $\mathbf{F_i} = (F_x^i, F_y^i, F_z^i, M_x^i, M_y^i, M_z^i)^T$, including forces and moments in six degrees of freedom, and $X_i = (dx_i, dy_i, dz_i, dx_i, dy_i, dz_i)^T$, including three translational and three rotational errors.

3.5. Yield Prediction

The tube is rejected in assembly if assembly loads exceed the maximum allowance. Therefore, to predict the assembly yield, we need to know the statistical distribution of the assembly loads. Having the preceding models, we can project the process errors into tube errors and then the assembly loads at each install point. Combining Eq (3), Eq (10) and Eq (11) we have

$$\mathbf{F} = \mathbf{K} * \mathbf{S} * \mathbf{V} + \mathbf{K} * \mathbf{U}' \qquad \text{Eq (12)}$$

$$E(\mathbf{F}) = \mathbf{K} * \mathbf{S} * E(\mathbf{V}) + \mathbf{K} * E(\mathbf{U}') \qquad \text{Eq (13)}$$

$$Var(\mathbf{F}) = (\mathbf{K} * \mathbf{S}) * Var(\mathbf{V}) * (\mathbf{K} * \mathbf{S})^T + \mathbf{K} * Var(\mathbf{U}') * \mathbf{K}^T \qquad \text{Eq (14)}$$

Where E(**F**) and Var(**F**) are the expected value vector and covariance matrix of **F** respectively. **F** is assumed to have a joint normal distribution and the probability density function of **F** can be expressed as

$$pdf(\mathbf{F}) = \frac{1}{\left(\sqrt{2p}\right)^{6h}\sqrt{|Var(\mathbf{F})|}} \exp\left(-\frac{1}{2}\mathbf{F}^T * Var(\mathbf{F})^{-1} * \mathbf{F}\right) \qquad \text{Eq (15)}$$

The assembly is acceptable only if the assembly loads are inside the allowance, such that

$$-\mathbf{F}_{\mathbf{MAX}} \le \mathbf{F} \le \mathbf{F}_{\mathbf{MAX}} \qquad \text{Eq (16)}$$

The yield of tube assembly **Y** is the probability that **F** falls inside the allowance. This is calculated through integrating the probability density function of **F**:

$$\mathbf{Y} = P(-\mathbf{F}_{\mathbf{MAX}} \le \mathbf{F} \le \mathbf{F}_{\mathbf{MAX}}) = \iint_{\mathbf{F}_{\mathbf{MAX}}} \cdots \int pdf(\mathbf{F}) dF_x^1 dF_y^1 \cdots dM_z^h \qquad \text{Eq (17)}$$

The covariation of **F** will make the integral in Eq (17) difficult as the dimension of **F** increases. An alternate method is using Monte Carlo simulation by generating many sets of random process errors, projecting them into assembly loads and checking if they exceed tolerance.

4. CASE STUDY

We demonstrate the methodology with the following example. As shown in Figure 12, a tube is designed to connect point 1 and 3 in the structure, and two geometry designs (I and II) are to be evaluated. Both designs have an intermediate tiedown (point 2).

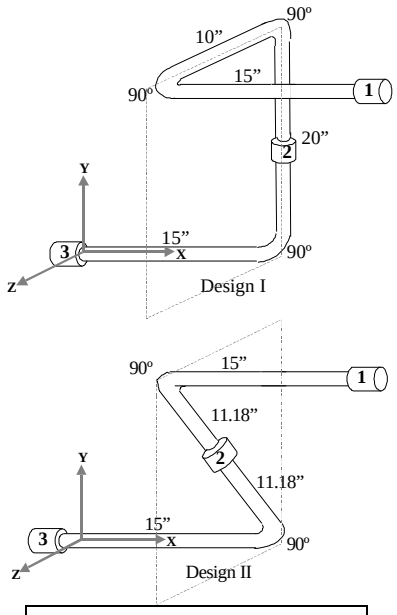

Specs & material properties:

ϕ1/2” Titanium Tube

Wall thickness: 1/32’

Elastic module E=1.60E+07psi

Shear module G=5.95E+06psi

Poison ratio=0.34

Figure 12: Two designs of tube in case study

The bend plans, statistics on process errors and assembly criteria are listed below.

4.1. Bending process parameters

The bend plan for design I comprises three cycles, and the bend plan for design II has two cycles. Their parameters are listed in Table 1.

Table 1: Bend plan for Design I and II

	Design I			Design II		
Bend cycle	*l*	*b*	*a*	*l*	*b*	*a*
1	15”	0 º	90 º	15”	0 º	90 º
2	10”	-90 º	90 º	22.36”	180 º	90 º
3	20”	-90 º	90 º			

The statistics on the process errors are listed in Table 2. Note that the process is centered without biases.

Table 2: Statistics on process errors

Process Errors	*l*	*b*	*a*
Mean	0	0	0
Standard Deviation	0.005”	0.1 ^{o}	0.1 ^{o}

4.2. Structural Variation and Assembly Criterion

There are three install points: two at the tips and one in the middle of the vertical section. The distributions of geometric variations **U’** on install points are unknown. However, their means are estimated to be zero and their standard deviations are estimated to be 0.1” for translational errors and 0.1^{o} for angular errors on both install points. The acceptance criterion for tube assembly is based on the assembly load, which requires that force in X, Y, Z directions at each install point cannot exceed 4 lbs. The minimum yield acceptable is 50%. If the yield is below that percentage, the tube must be redesigned.

4.3. Yield Prediction

The derivation of sensitivity matrices and stiffness matrices for Design I and II is shown in the Appendix. Using Monte Carlo simulation for both designs, we can predict the yields in tube assembly under different levels of the structure variation **U’** by counting the percentage of assembly loads that exceeds the 4 lbs allowance. The results are plotted in Figure 13. For Design I, the maximum yield is 99% when no structure variations exist, i.e., the only effect is the tube variations. The yield declines as the structure variations increase, and reaches 76% at the estimated structure variation **U’**. The yield hits the minimum acceptable yield of 50% at 1.7**U’**, which is the maximum level of structure variations the tube can absorb. For Design II, the maximum yield is 97% without structure variations. The yield declines rapidly as the structure variations increase, falling below 50% at 0.3**U’**. At the estimated structure variation **U’**, the yield is only 5%.

The results shows that Design I is more robust in that it is less sensitive to the uncertainty of variations and has higher yield in any scenario. This is because Design II is stiffer than Design I even though its tube variation is smaller due to fewer bends. Similar iterations can be repeated to optimize the tube design, as well as to test the effectiveness of different yield improvement options. Such options include material/specification change, variation reduction in bending process, variation reduction in mating structure, and load allowance relaxation.

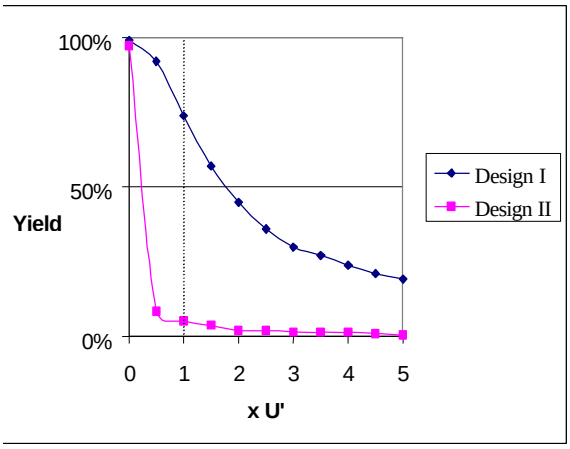

Figure 13: Assembly yields of the two designs under different levels of structure variations

5. CONCLUSION

This paper demonstrates an analytical approach to predict the geometrical variation and compliance of tubes, and the assembly yield. This approach significantly reduces the dependency on simulation and computational efforts. A case study demonstrates how this methodology can assist design optimization and explore alternatives in yield improvement.

Several issues need to be addressed in ongoing research. First, an optimization algorithm needs to be applied to tube design, so that process sensitivity can be minimized and compliance can be maximized. Second, in-process inspection needs to be incorporated into the model. The allocation of dimensional tolerances for inspection needs to be optimized, so that its conformance to the acceptance criteria in assembly is maximized. Finally, for the optimum yield improvement scheme, the overall optimization framework incorporating costs and performance measures at system level needs to be developed.

ACKNOWLEDGEMENTS

This material is based upon work supported by Boeing Co. and National Science Foundation Career Award Grant No. 9702662.

REFERENCE

1. Asada, H. and Slotine, J.-J. E. (1986) *Robot Analysis and Control*. John Wiley & Sons, Inc., New York.
2. Bjorke, O. (1978) *Computer Aided Tolerancing*, Tapir Publication, Trondheim, Norway
3. Chang, M. (1996) *Modeling the Assembly of Compliant, Non-Ideal Parts.* Ph.D. Thesis. MIT, Boston
4. Cook R.D. and Young, W.C. (1985) *Advanced Mechanics of Materials.* McMillan Publishing Co., New York.
5. Cook, N. (1984) *Mechanics and Materials for Design.* McGraw-Hill Book Co., New York.

6. Daniel, F., Weil R., and Bourdet, P. (1986) “Computer Aided Tolerancing and Dimensioning in Process Planning” *CIRP Annals*, Vol. 35/1, pp. 381-386
7. Frank, B. (1993) “Pipe and Tube Bending: a Refresher Course.” *Welding Design & Fabrication*. V. 66, June 1993, p. 72-73
8. Frey, D. D. (1997) *Using Product Tolerances to Drive Manufacturing System Design*. Ph.D. Thesis. MIT, Boston.
9. Fritzinger, D. (1997) “A Quick Course in Bending Tubes. ” *Machine Design*. V. 69, Mar. 20 1997, p. 67-8.
10. Guilford, J. and Turner, J.U. (1993) “Advances Tolerance Analysis and Synthesis for Geometric Tolerances” *ASME Manufacturing Review*, December
11. Hu, S.J. (1997) “Stream-of-Variation Theory for Automotive Body Assembly.” *CIRP Annals* V. 46(1) 1997, p. 1-6
12. Kazmer, D., P. Barkan, et al. (1996) “Quantifying Design and Manufacturing Robustness Through Stochastic Optimization Techniques” *ASME Design Automation Conference*, Irvine, CA, ASME
13. Liu, S.C. and Hu, S.J. (1997) “Variation Simulation for Deformable Sheet Metal Assemblies Using Finite Element Methods” *Transactions of the ASME Journal of Manufacturing Science and Engineering*, Vol. 119, pp. 368-374, August
14. Pilkey, W. (1994) *Formulas for Stress, Strain, and Structural Matrices*. John Wiley & Sons, Inc., New York.
15. Shimano, B.E. (1978) *The Kinematic Design and Force Control of Computer Controlled Manipulators.* Ph.D. Thesis. Stanford University, Stanford, CA.
16. Slocum, A. H. (1992) *Precision Machine Design*. Prentice Hall, Inc., New Jersey.
17. Soman, N.A. (1996) *A Model of the Assembly of Compliant Parts.* Ph.D. Thesis. MIT, Boston
18. Suri, R. and Otto, K. (1999) “Variation Modeling for Sheet Stretch Forming Manufacturing System” *Annals of CIRP*.
19. Szykman, S, Cagan, J (1996) “Synthesis of Optimal Non-orthogonal Routes” *Journal of Mechanical Design* Vol. 118, No. 3, pp. 419-424 September
20. Szykman, S, Cagan, J and Weisser, P (1998) “An Integrated Approach to Optimal Three Dimensional Layout and Routing” *Journal of Mechanical Design* Vol. 120, No. 3, pp. 510-512 September
21. Takahashi, K., Suzuki, H., and Kimura, F. (1991) “Tolerance Analysis in Machine Assembly by Classifying Part Contact State” *Proceedings of CIRP Seminar on Computer Aided Tolerancing*, pp. 57-76
22. Turner, J.U. (1990) “Relative Positioning of Parts in Assemblies using Mathematical Programming” *Computer-Aided Design*, vol. 22, no. 7, pp. 394-400, September
23. Turner, J.U. and Gangoiti, A.B. (1991) “Tolerance Analysis Approaches in Commercial Software” *Concurrent Engineering Issues, Technology, and Practice*, Vol. 1, No. 2, pp. 11-23, March
24. Veitschegger, W.K. and Wu, C.H. (1986) “Robot Accuracy Analysis Based on Kinematics.” *IEEE Journal of Robotics and Automation* V. RA-2, No. 3, September 1986, p. 171-179
25. Whitney, D., Gilbert, O.L. and Jastrzebski, M. (1994) “Representation of Geometric Variation Using Matrix Transforms for Statistical Tolerance Analysis in Assembly” *Research in Engineering Design* V. 6 1994, p. 51-70

APPENDIX

Variation propagation in case study

Design I: Let the process errors in the three bend cycles be $d\mathbf{l}=(dl_1 \;\; dl_2 \;\; dl_3)^T$, $d\mathrm{a}=(da_1 \;\; da_2 \;\; da_3)^T$ and $d\mathrm{b}=(db_1, \; db_2, \; db_3)^T$. Assuming install point 3 is fixed, let the geometrical errors at install point 1 be $d\mathbf{P_2}=(dx_1, \; dy_1, \; dz_1)^T$ and $\mathrm{d_1}=(dx_1, \; dy_1, \; dz_1)^T$. Similarly, let the geometrical errors at install point 2 be $d\mathbf{P_2}=(dx_2, \; dy_2, \; dz_2)^T$ and $\mathrm{d_2}=(dx_2, \; dy_2, \; dz_2)^T$. Note that all angles are in radians. Through the procedures in Section 0 we derive the individual variation propagation equations as follows:

$$\begin{pmatrix} dx_1 \\ dy_1 \\ dz_1 \\ dx_1 \\ dy_1 \\ dz_1 \end{pmatrix} = \begin{pmatrix} 1 & 0 & 0 & 0 & 0 & -20 & 0 & 0 & -10 \\ 0 & 0 & 1 & 0 & -10 & 15 & 0 & -15 & 0 \\ 0 & 1 & 0 & -15 & 0 & 0 & 0 & 0 & 15 \\ 0 & 0 & 0 & 0 & 1 & 0 & -1 & 0 & 0 \\ 0 & 0 & 0 & 1 & 0 & 0 & 0 & 0 & -1 \\ 0 & 0 & 0 & 0 & 0 & 1 & 0 & -1 & 0 \end{pmatrix} * \begin{pmatrix} dl_1 \\ dl_2 \\ dl_3 \\ da_1 \\ da_2 \\ da_3 \\ db_1 \\ db_2 \\ db_3 \end{pmatrix}$$

$$\begin{pmatrix} dx_2 \\ dy_2 \\ dz_2 \\ dx_2 \\ dy_2 \\ dz_2 \end{pmatrix} = \begin{pmatrix} 0 & -10 & 0 \\ 1 & 0 & 0 \\ 0 & 0 & 0 \\ 0 & 0 & 0 \\ 0 & 0 & -1 \\ 0 & 1 & 0 \end{pmatrix} * \begin{pmatrix} dl_3 \\ da_3 \\ db_3 \end{pmatrix}$$

Combining them together, we can obtain the overall variation propagation equation:

$$\begin{pmatrix} dx_1 \\ dy_1 \\ dz_1 \\ dx_1 \\ dy_1 \\ dz_1 \\ dx_2 \\ dy_2 \\ dz_2 \\ dx_2 \\ dy_2 \\ dz_2 \end{pmatrix} = \begin{pmatrix} 1 & 0 & 0 & 0 & 0 & -20 & 0 & 0 & -10 \\ 0 & 0 & 1 & 0 & -10 & 15 & 0 & -15 & 0 \\ 0 & 1 & 0 & -15 & 0 & 0 & 0 & 0 & 15 \\ 0 & 0 & 0 & 0 & 1 & 0 & -1 & 0 & 0 \\ 0 & 0 & 0 & 1 & 0 & 0 & 0 & 0 & -1 \\ 0 & 0 & 0 & 0 & 0 & 1 & 0 & -1 & 0 \\ 0 & 0 & 0 & 0 & 0 & -10 & 0 & 0 & 0 \\ 0 & 0 & 1 & 0 & 0 & 0 & 0 & 0 & 0 \\ 0 & 0 & 0 & 0 & 0 & 0 & 0 & 0 & 0 \\ 0 & 0 & 0 & 0 & 0 & 0 & 0 & 0 & 0 \\ 0 & 0 & 0 & 0 & 0 & 0 & 0 & 0 & -1 \\ 0 & 0 & 0 & 0 & 0 & 1 & 0 & 0 & 0 \end{pmatrix} * \begin{pmatrix} dl_1 \\ dl_2 \\ dl_3 \\ da_1 \\ da_2 \\ da_3 \\ db_1 \\ db_2 \\ db_3 \end{pmatrix}$$

Design II: Design II has only two bends. Through a similar process, we have

$$\begin{pmatrix} dx_1 \\ dy_1 \\ dz_1 \\ dx_1 \\ dy_1 \\ dz_1 \\ dx_2 \\ dy_2 \\ dz_2 \\ dx_2 \\ dy_2 \\ dz_2 \end{pmatrix} = \begin{pmatrix} 1 & 0 & 0 & -22.36 & 0 & 0 \\ 0 & 0.89 & -13.42 & 0 & 0 & -6.71 \\ 0 & 0.45 & -6.71 & 0 & 0 & 13.42 \\ 0 & 0 & 0 & 0 & -1 & 0 \\ 0 & 0 & 0.45 & -0.45 & 0 & -0.89 \\ 0 & 0 & -0.89 & 0.89 & 0 & -0.45 \\ 0 & 0 & 0 & -11.18 & 0 & 0 \\ 0 & 0.89 & 0 & 0 & 0 & 0 \\ 0 & 0.45 & 0 & 0 & 0 & 0 \\ 0 & 0 & 0 & 0 & 0 & 0 \\ 0 & 0 & 0 & -0.45 & 0 & -0.89 \\ 0 & 0 & 0 & 0.89 & 0 & -0.45 \end{pmatrix} * \begin{pmatrix} dl_1 \\ dl_2 \\ da_1 \\ da_2 \\ db_1 \\ db_2 \end{pmatrix}$$

Characteristic stiffness matrices:

The characteristic stiffness matrix that relates the generalized forces and displacements at the three install points is derived:

Design I:

$$K = \begin{pmatrix}
8.12E+01 & 6.32E+00 & 1.96E+01 & -1.82E+00 & 4.20E+01 & -2.04E+01 & -8.12E+01 & -6.32E+00 & -1.96E+01 & -1.10E+02 & -1.31E+02 & 5.13E+02 \\
6.32E+00 & 3.30E+01 & 4.61E+00 & 4.53E+01 & 3.42E+01 & -3.33E+02 & -6.32E+00 & -3.30E+01 & -4.61E+00 & 5.45E+01 & -4.09E+00 & -1.95E+01 \\
1.96E+01 & 4.61E+00 & 4.13E+01 & -1.59E+01 & 3.82E+02 & -3.57E+01 & -1.96E+01 & -4.61E+00 & -4.13E+01 & -2.55E+02 & 3.61E+01 & 1.18E+02 \\
-1.82E+00 & 4.53E+01 & -1.59E+01 & 5.98E+02 & -1.59E+02 & -4.66E+02 & 1.82E+00 & -4.53E+01 & 1.59E+01 & -3.06E+02 & -2.52E+01 & -9.07E+01 \\
4.20E+01 & 3.42E+01 & 3.82E+02 & -1.59E+02 & 4.34E+03 & -3.22E+02 & -4.20E+01 & -3.42E+01 & -3.82E+02 & -2.38E+03 & 7.20E+01 & 2.07E+02 \\
-2.04E+01 & -3.33E+02 & -3.57E+01 & -4.66E+02 & -3.22E+02 & 3.92E+03 & 2.04E+01 & 3.33E+02 & 3.57E+01 & -6.14E+02 & -2.43E+01 & -7.41E+01 \\
-8.12E+01 & -6.32E+00 & -1.96E+01 & 1.82E+00 & -4.20E+01 & 2.04E+01 & 3.03E+02 & 3.95E+01 & 1.96E+01 & 1.10E+02 & 1.31E+02 & 7.54E+02 \\
-6.32E+00 & -3.30E+01 & -4.61E+00 & -4.53E+01 & -3.42E+01 & 3.33E+02 & 3.95E+01 & 9.05E+01 & 4.61E+00 & -5.45E+01 & 4.09E+00 & 6.10E+01 \\
-1.96E+01 & -4.61E+00 & -4.13E+01 & 1.59E+01 & -3.82E+02 & 3.57E+01 & 1.96E+01 & 4.61E+00 & 8.04E+01 & 7.89E+00 & 5.93E+01 & -1.18E+02 \\
-1.10E+02 & 5.45E+01 & -2.55E+02 & -3.06E+02 & -2.38E+03 & -6.14E+02 & 1.10E+02 & -5.45E+01 & 7.89E+00 & 4.56E+03 & -8.54E+02 & -8.12E+02 \\
-1.31E+02 & -4.09E+00 & 3.61E+01 & -2.52E+01 & 7.20E+01 & -2.43E+01 & 1.31E+02 & 4.09E+00 & 5.93E+01 & -8.54E+02 & 1.85E+03 & -8.45E+02 \\
5.13E+02 & -1.95E+01 & 1.18E+02 & -9.07E+01 & 2.07E+02 & -7.41E+01 & 7.54E+02 & 6.10E+01 & -1.18E+02 & -8.12E+02 & -8.45E+02 & 1.24E+04 \\
 & & & & & & -2.22E+02 & -3.32E+01 & 7.70E-07 & -1.29E-11 & -2.94E-05 & -1.27E+03 \\
 & & & & & & -3.32E+01 & -5.75E+01 & 4.28E-07 & 5.74E-06 & -3.18E-06 & -4.15E+01 \\
 & & & & & & 7.70E-07 & 4.28E-07 & -3.90E+01 & 2.47E+02 & -9.54E+01 & 3.18E-06 \\
 & & & & & & 2.53E-11 & -6.07E-07 & -2.62E+01 & -5.25E+02 & -5.75E+01 & 1.34E-06 \\
 & & & & & & -2.60E-06 & -2.92E-06 & 3.73E+02 & -2.36E+03 & 1.78E+02 & -6.82E-06 \\
 & & & & & & -1.12E+02 & -4.99E+02 & 2.92E-06 & 5.47E-05 & -6.82E-06 & -1.16E+02
\end{pmatrix}$$

$$\begin{pmatrix}
-2.22E+02 & -3.32E+01 & 7.70E-07 & -2.94E-05 & -3.18E-06 & -9.54E+01 & -5.75E+01 \\
-3.32E+01 & -5.75E+01 & 4.28E-07 & -3.90E+01 & 2.62E+01 & 7.08E+02 & -2.57E+02 \\
7.70E-07 & 4.28E-07 & -3.90E+01 & 2.47E+02 & -9.54E+01 & 3.18E-06 & -7.70E-07 \\
2.53E-11 & -6.07E-07 & -2.62E+01 & -5.25E+02 & -5.75E+01 & 1.34E-06 & -2.53E-11 \\
-2.60E-06 & -2.92E-06 & 3.73E+02 & -2.36E+03 & 1.78E+02 & -6.82E-06 & 2.60E-06 \\
-1.12E+02 & -4.99E+02 & 2.92E-06 & 5.47E-05 & -6.82E-06 & -1.16E+02 & 1.12E+02
\end{pmatrix}$$

$$\begin{pmatrix}
-2.22E+02 & -3.32E+01 & 7.70E-07 & 2.86E-11 \\
-3.32E+01 & -5.75E+01 & 4.28E-07 & -6.07E-07 \\
7.70E-07 & 4.28E-07 & -3.90E+01 & -2.62E+01 \\
-2.53E-11 & 6.07E-07 & 2.62E+01 & 7.08E+02 \\
2.92E-06 & -3.73E+02 & -2.57E+02 & 5.95E-06 \\
4.99E+02 & -2.92E-06 & 5.95E-06 &
\end{pmatrix}$$

Design II:

$$K = \begin{pmatrix}
1.50E+02 & 2.68E+01 & 1.34E+01 & -4.64E-06 & 4.59E+01 & -9.19E+01 & -1.50E+02 & -2.68E+01 & -1.34E+01 & -1.15E-05 & -4.34E+02 & 8.68E+02 \\
2.68E+01 & 5.28E+01 & 9.02E+00 & 1.46E+01 & 6.46E+01 & -4.66E+02 & -2.68E+01 & -5.28E+01 & -9.02E+00 & 1.13E+02 & -5.46E+01 & 2.88E+01 \\
1.34E+01 & 9.02E+00 & 3.93E+01 & -2.92E+01 & 3.70E+02 & -6.46E+01 & -1.34E+01 & -9.02E+00 & -3.93E+01 & -2.25E+02 & 5.31E+01 & 5.46E+01 \\
-2.11E-05 & 1.46E+01 & -2.92E+01 & 6.95E+02 & -2.88E+02 & -1.44E+02 & 2.11E-05 & -1.46E+01 & 2.92E+01 & -4.27E+02 & -6.22E+01 & -3.11E+01 \\
4.59E+01 & 6.46E+01 & 3.70E+02 & -2.88E+02 & 4.23E+03 & -5.42E+02 & -4.59E+01 & -6.46E+01 & -3.70E+02 & -2.18E+03 & 3.30E+01 & 1.04E+02 \\
-9.19E+01 & -4.66E+02 & -6.46E+01 & -1.44E+02 & -5.42E+02 & 5.05E+03 & 9.19E+01 & 4.66E+02 & 6.46E+01 & -1.09E+03 & 1.04E+02 & -1.23E+02 \\
-1.50E+02 & -2.68E+01 & -1.34E+01 & 4.64E-06 & -4.59E+01 & 9.19E+01 & 3.00E+02 & 5.37E+01 & 2.68E+01 & 1.50E-06 & -3.82E-04 & 5.67E-04 \\
-2.68E+01 & -5.28E+01 & -9.02E+00 & -1.46E+01 & -6.46E+01 & 4.66E+02 & 5.37E+01 & 1.06E+02 & 1.80E+01 & 6.22E-07 & 1.42E-04 & -3.12E-04 \\
-1.34E+01 & -9.02E+00 & -3.93E+01 & 2.92E+01 & -3.70E+02 & 6.46E+01 & 2.68E+01 & 1.80E+01 & 7.86E+01 & -3.48E-05 & 1.55E-04 & -1.32E-05 \\
-2.72E-05 & 1.13E+02 & -2.25E+02 & -4.27E+02 & -2.18E+03 & -1.09E+03 & 5.06E-06 & -4.49E-05 & 4.40E-05 & 4.98E+03 & -1.05E+03 & -5.26E+02 \\
-4.34E+02 & -5.46E+01 & 5.31E+01 & -6.22E+01 & 3.30E+01 & 1.04E+02 & -3.78E-04 & 7.68E-05 & 2.28E-04 & -1.05E+03 & 4.38E+03 & -5.25E+03 \\
8.68E+02 & 2.88E+01 & 5.46E+01 & -3.11E+01 & 1.04E+02 & -1.23E+02 & 5.57E-04 & -3.16E-04 & 1.13E-05 & -5.26E+02 & -5.25E+03 & 1.23E+04 \\
 & & & & & & -1.50E+02 & -2.68E+01 & -1.34E+01 & 9.98E-06 & 4.34E+02 & -8.68E+02 \\
 & & & & & & -2.68E+01 & -5.28E+01 & -9.02E+00 & -1.13E+02 & 5.46E+01 & -2.88E+01 \\
 & & & & & & -1.34E+01 & -9.02E+00 & -3.93E+01 & 2.25E+02 & -5.31E+01 & -5.46E+01 \\
 & & & & & & 8.20E-05 & 1.46E+01 & -2.92E+01 & -4.27E+02 & -6.22E+01 & -3.11E+01 \\
 & & & & & & 4.59E+01 & 6.46E+01 & 3.70E+02 & -2.18E+03 & 3.30E+01 & 1.04E+02 \\
 & & & & & & -9.19E+01 & -4.66E+02 & -6.46E+01 & -1.09E+03 & 1.04E+02 & -1.23E+02
\end{pmatrix}$$

$$\begin{pmatrix}
-1.50E+02 & -2.68E+01 & -1.34E+01 & 7.28E-05 \\
-2.68E+01 & -5.28E+01 & -9.02E+00 & 1.46E+01 \\
-1.34E+01 & -9.02E+00 & -3.93E+01 & -2.92E+01 \\
-2.72E-05 & 1.13E+02 & -2.25E+02 & -4.27E+02 \\
-4.34E+02 & -5.46E+01 & 5.31E+01 & -6.22E+01 \\
8.68E+02 & 2.88E+01 & 5.46E+01 & -3.11E+01 \\
1.50E+02 & 2.68E+01 & 1.34E+01 & -7.28E-05 \\
2.68E+01 & 5.28E+01 & 9.02E+00 & -1.46E+01 \\
1.34E+01 & 9.02E+00 & 3.93E+01 & 2.92E+01 \\
-8.20E-05 & -1.46E+01 & 2.92E+01 & 6.95E+02 \\
-4.59E+01 & -6.46E+01 & -3.70E+02 & -2.88E+02 \\
9.19E+01 & 4.66E+02 & 6.46E+01 & -1.44E+02
\end{pmatrix}$$